

RESEARCH ARTICLE | FEBRUARY 13 2024

Correlation-induced viscous dissipation in concentrated electrolytes ^{EP}

Special Collection: [2024 JCP Emerging Investigators Special Collection](#)

Paul Robin  

 Check for updates

J. Chem. Phys. 160, 064503 (2024)

<https://doi.org/10.1063/5.0188215>



CrossMark



The Journal of Chemical Physics
Special Topic: Time-resolved
Vibrational Spectroscopy

Submit Today



Correlation-induced viscous dissipation in concentrated electrolytes

Cite as: J. Chem. Phys. 160, 064503 (2024); doi: 10.1063/5.0188215

Submitted: 20 November 2023 • Accepted: 21 January 2024 •

Published Online: 13 February 2024



View Online



Export Citation



CrossMark

Paul Robin^{a)} 

AFFILIATIONS

Laboratoire de Physique de l'École Normale Supérieure, ENS, Université PSL, CNRS, Sorbonne Université, Université Paris-Diderot, Sorbonne Paris Cité, Paris, France and Institute of Science and Technology Austria, 3400 Klosterneuburg, Austria

Note: This paper is part of the 2024 JCP Emerging Investigators Special Collection.

^{a)} Author to whom correspondence should be addressed: paul.robin@ista.ac.at

ABSTRACT

Electrostatic correlations between ions dissolved in water are known to impact their transport properties in numerous ways, from conductivity to ion selectivity. The effects of these correlations on the solvent itself remain, however, much less clear. In particular, the addition of salt has been consistently reported to affect the solution's viscosity, but most modeling attempts fail to reproduce experimental data even at moderate salt concentrations. Here, we use an approach based on stochastic density functional theory, which accurately captures charge fluctuations and correlations. We derive a simple analytical expression for the viscosity correction in concentrated electrolytes, by directly linking it to the liquid's structure factor. Our prediction compares quantitatively to experimental data at all temperatures and all salt concentrations up to the saturation limit. This universal link between the microscopic structure and viscosity allows us to shed light on the nanoscale dynamics of water and ions under highly concentrated and correlated conditions.

© 2024 Author(s). All article content, except where otherwise noted, is licensed under a Creative Commons Attribution (CC BY) license (<http://creativecommons.org/licenses/by/4.0/>). <https://doi.org/10.1063/5.0188215>

I. INTRODUCTION

One mole of table salt is dissolved in a liter of pure water: how does this addition modify the liquid's viscosity? While this question has been addressed in great detail by many experimentalists over the past two centuries,^{1–3} their observations are often difficult to rationalize beyond the qualitative level. In particular, the effects of electrostatic interactions between ions dissolved in water are known to be manifold, with unclear consequences on the liquid's rheological properties. How these interactions impact ions' transport properties has been the subject of many modeling attempts for over a century, starting with the seminal studies of Debye, Hückel, Onsager, and others.^{4–6} Most existing theories of electrokinetic transport share, however, many common shortcomings, such as failing at high salt concentrations or for multivalent ions. In addition, the exact nature of the coupling between the motion of dissolved ions and that of the surrounding solvent remains a very much open question, even in the apparently simple case of ions in room temperature water, let alone more complex environments, such as

nanoconfined or glass-forming liquids,^{7–9} where charge fluctuations can play a key role.¹⁰

Here, we focus on the impact of the presence of salt on the liquid's viscosity. It had, indeed, be noticed first by Poiseuille¹ that increasing the salt concentration generally also increases an electrolyte's viscosity, sometimes by up to one order of magnitude near the saturation limit. Later, Jones and Dole³ noted that, in most cases, the relative change in the liquid's viscosity η followed an empirical law—now known as the Jones–Dole equation—of the form

$$\Delta\eta = \eta - \eta_0 \simeq A\sqrt{c} + Bc, \quad (1)$$

where η_0 is the viscosity of the pure solvent at the same temperature, c is the salt concentration, and A and B are empirical salt- and temperature-dependent parameters.

From the qualitative point of view, the origin of this “ionic viscosity” can be readily understood. At thermal equilibrium, ions

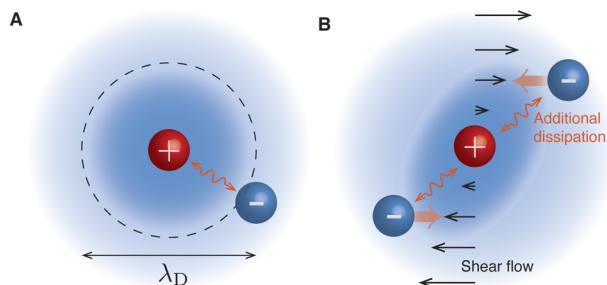


FIG. 1. Electrostatic correlations in aqueous electrolytes. (a) Debye correlation cloud around a cation at thermal equilibrium. (b) Deformation of the correlation cloud under a shear flow, in the reference frame of a cation. This deformation allows ions to transmit momentum through the fluid via electrostatic interactions, playing the role of an additional viscosity.

are typically surrounded by oppositely charged ions, creating the so-called Debye correlation cloud extending over a typical scale known as the Debye length [see Fig. 1(a)],

$$\lambda_D = \sqrt{\frac{\epsilon k_B T}{2e^2 c}}, \quad (2)$$

where T is the temperature, ϵ is the solvent's dielectric constant, k_B is Boltzmann's constant, and e is the elementary charge. In the presence of a fluid velocity gradient, however, the correlation cloud is sheared [see Fig. 1(b)], and electrostatic forces between ions contribute to homogenize momentum throughout the fluid, effectively increasing its viscosity. Quantifying this effect is a notoriously hard problem, pioneered by Falkenhagen and co-workers.¹¹ They obtained that, in the limit of infinite dilution, ion–ion electrostatic interactions are responsible for a viscosity increase of the form

$$\Delta\eta_{\text{ion-ion}} = \frac{1}{60} \frac{\sqrt{\ell_B c} k_B T}{\sqrt{8\pi} D}, \quad (3)$$

where we introduced the diffusion coefficient D of ions as well as the Bjerrum length ℓ_B , which measures the strength of electrostatic interactions,

$$\ell_B = \frac{e^2}{4\pi\epsilon k_B T}. \quad (4)$$

This result yields a theoretical prediction for the value of the coefficient A of the Jones–Dole equation (1). This prediction compares favorably to experiments in the limit of a very high dilution (see Fig. 2).

At higher concentrations, the B term introduced by Jones and Dole is generally interpreted as describing how individual ions perturb the solvent—an effect that is *a priori* linear with salt concentration. It was initially believed that ions that reinforce the hydrogen bond network of water (known as kosmotropes) were associated with positive values of B and ions that weaken it (chaotropes) with negative values. Yet, recent studies have shown that, while this effect does seem to originate in local electrostatic interactions between ions and water, it does not correspond to large-scale changes in the

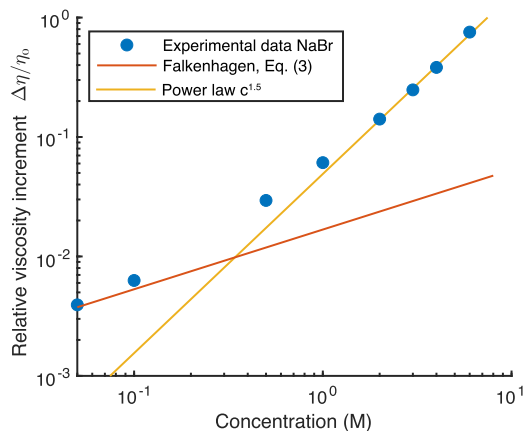


FIG. 2. Comparison between experimental data and the Falkenhagen limiting law. Blue points: Experimental data for a NaBr solution at 25 °C. [Reproduced with permission from Isono, J. Chem. Eng. Data **29**, 45–52 (1984). Copyright 1984 American Chemical Society.] Red line: Falkenhagen limiting law, $\Delta\eta \propto \sqrt{c}$. Yellow line: Power law fit $\Delta\eta \propto c^{1.5}$ in the limit of high concentrations.

solvent's structure.^{12,13} In addition, adding this phenomenological term only provides a good agreement with experimental data for concentrations up to around 100 mM.

Based on these observations, one can write the viscosity increment as the sum of two terms,

$$\Delta\eta = \Delta\eta_{\text{ion-ion}} + \Delta\eta_{\text{ion-water}}, \quad (5)$$

where $\Delta\eta_{\text{ion-ion}}$ (respectively, $\Delta\eta_{\text{ion-water}}$) corresponds to the contribution of ion–ion (respectively, ion–water) interactions.

Various attempts at extending the Jones–Dole law were reported in the literature;^{15–17} they generally amount to adding phenomenological terms scaling as c^2 , $c \log c$, etc., emerging from, for example, volume exclusion effects, ion–ion interactions, or electrostatic barriers for microscopic rearrangements—without strong theoretical evidence for any of the suggested scalings. In addition, the suggested models contain various fitting parameters that do not allow for easy physical interpretation, or only compare reasonably to certain salts or experimental conditions. As an example of such limitations, in the limit of very high concentrations (above 1M), the viscosity increment seems to scale as $c^{3/2}$; see Fig. 2 in the case of sodium bromide (NaBr). This scaling differs from the ones often used in the literature to extend the Jones–Dole law.

It is not *a priori* clear whether these high-concentration deviations arise from ion–ion or ion–water interactions. However, rescaling the viscosity increment by the viscosity of pure water $\eta_0(T)$, and plotting it as a function of the quantity $c\ell_B$, experimental data for a given salt at all temperatures seem to collapse on a single master curve at high concentrations (see Fig. 3). Since $c\ell_B \propto \lambda_D^{-2}$ is a measure of electrostatic correlations between ions, this observation suggests that high concentration deviations arise mostly from ion–ion interactions.

Based on these observations, we develop in this paper a field-theoretical approach for the description of this ionic viscosity and show that it can be directly determined from the charge structure

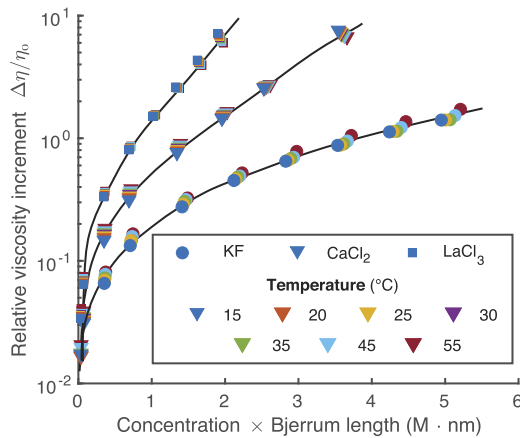


FIG. 3. Rescaled viscosity increment as a function of concentration and temperature. x axis: $c \times \ell_B$ (note that ℓ_B depends on temperature); y axis: $\Delta\eta/\eta_0(T)$. The symbols represent experimental data for KF, CaCl_2 , and LaCl_3 . [Reproduced with permission from Isono, J. Chem. Eng. Data **29**, 45–52 (1984). Copyright 1984 American Chemical Society and Goldsack and Franchetto, Can. J. Chem. **56**, 1442–1450 (1978). Copyright 1978 Canadian Science Publishing.] Colors represent temperatures. Black lines are a guide to the eye.

factor of the electrolyte. The latter can be determined, thanks to a stochastic density functional theory based on the Dean–Kawasaki equation,^{19,20} which has recently proved successful at determining various properties of electrolytes.^{21–24} In particular, we make use of a technique introduced by Avni and co-workers²² to cut off electrostatic interactions at short distances, enabling to better describe the structure of concentrated electrolytes.

Overall, we show as our main result that the viscosity increment can be determined analytically as a Fourier space integral,

$$\Delta\eta_{\text{ion-ion}} = \frac{c}{15(2\pi)^2} \frac{k_B T}{D} \int dq V(q) \frac{d}{dq} \left[q^2 C_\rho^0(q) \frac{\partial C_\rho^0}{\partial q} \right], \quad (6)$$

where $V(q)$ is the Fourier-transformed ion–ion interaction potential (e.g., electrostatic or van der Waals interactions) and C_ρ^0 is the charge structure factor of the electrolyte at thermal equilibrium in the absence of any flow—directly linking the electrolyte’s microscopic structure to a macroscopic quantity such as viscosity. Based on this result, a simple *Ansatz* for the viscosity of concentrated electrolytes is found to be

$$\Delta\eta = B(T)c + \frac{1}{60\sqrt{8\pi}} \frac{k_B T}{D} \left[\sqrt{\ell_B c} + 6\pi a^2 (\ell_B c)^{3/2} \right], \quad (7)$$

where the only new parameter introduced by our model is the ionic size a , allowing for straightforward physical interpretation. We show that this theoretical result compares favorably to experimental data under nearly all conditions of temperature, concentration, salt composition, and valence and can correctly predict viscosity increments of more than 300%, in the case of multivalent salts close to the saturation limit.

This paper is organized as follows: in Sec. II, we present our field-theoretical framework and derive Eq. (7). Readers not interested in the details of the computation may skip Secs. II B–II F

and go directly to Sec. III, where we compare our predictions to a large body of experimental data. We also provide a simple, quantitative interpretation of our result. Finally, Sec. IV establishes our conclusion.

II. FROM ELECTROSTATIC CORRELATIONS TO THE IONIC VISCOSITY

A. Hydrodynamics with ions

We consider an aqueous solution containing some monovalent binary salt X^+, Y^- with concentration c , subjected to a shear flow. We only consider ion–ion interactions and, therefore, treat water as a continuous fluid with a given permittivity $\epsilon(T)$. We assume that both types of ions are monovalent with the same diffusion coefficient D and have the same physical size; the relaxation of these assumptions will be discussed later. We denote by $\mathbf{u}(\mathbf{r})$ the local fluid velocity, $p(\mathbf{r})$ the pressure field, $n_+(\mathbf{r})$ the local density in cations, and $n_-(\mathbf{r})$ the local density in anions. We define $\rho(\mathbf{r}) = n_+(\mathbf{r}) - n_-(\mathbf{r})$ the local charge density. It should be noted that $\langle \rho \rangle = 0$ due to electroneutrality and that $\langle n_+ \rangle = \langle n_- \rangle = c$. In the limit of low Reynolds numbers, the velocity field solves the Stokes equation,

$$\eta_0 \nabla^2 \mathbf{u} - \nabla p + \mathbf{f}(\mathbf{r}) = 0, \quad (8)$$

where \mathbf{f} represents all body forces acting on the fluid, other than pressure. If the fluid is subject to no external force, then $\mathbf{f}(\mathbf{r})$ corresponds only to interactions between dissolved ions at position \mathbf{r} and other ions elsewhere, which derives from an interaction potential $V(r)$,

$$\mathbf{f}(\mathbf{r}) = -k_B T \int d\mathbf{r}' \rho(\mathbf{r}) \nabla V(\mathbf{r} - \mathbf{r}') \rho(\mathbf{r}'). \quad (9)$$

In the simplest case, where we assume that ions are point particles with no short-range repulsion, the interaction potential is simply the Coulomb potential: $V(\mathbf{r}) = e^2/4\pi k_B T \epsilon r = \ell_B/r$. Other situations will also be addressed later. Since the fluid is electroneutral on average, $\langle \rho \rangle = 0$ and the net force $\langle \mathbf{f} \rangle$ acting on the fluid is solely due to local and random charge fluctuations. Introducing the Fourier transform as

$$\mathbf{f}(\mathbf{k}) = \int d\mathbf{r} \mathbf{f}(\mathbf{r}) e^{i\mathbf{k}\cdot\mathbf{r}}, \quad (10)$$

we can express the electrostatic force as

$$\langle \mathbf{f}(\mathbf{k}) \rangle = \frac{k_B T}{(2\pi)^3} \int d\mathbf{q} \langle \rho(\mathbf{k} - \mathbf{q}) \rho(\mathbf{q}) \rangle (i\mathbf{q}) V(q). \quad (11)$$

This force vanishes at equilibrium due to the problem’s symmetries but may take a non-zero value in the presence of an external shear flow. The last equation allows us to directly link $\langle \mathbf{f} \rangle$ to the electrolyte’s charge structure factor defined as

$$\Gamma_\rho(\mathbf{k}, \mathbf{k}') = \langle \rho(\mathbf{k}) \rho(\mathbf{k}') \rangle. \quad (12)$$

The goal of Secs. II B–II F is, therefore, to compute this structure factor using a field-theoretical approach and to use Eq. (11) to show that

$$\langle \mathbf{f}(\mathbf{k}) \rangle \simeq -k^2 \Delta\eta \mathbf{u}(\mathbf{k}). \quad (13)$$

To do so, we first compute the structure factor Γ_ρ at equilibrium (i.e., in the absence of any flow) and use it to compute the effect of advection by the solvent when an external flow is present. We then deduce a first-order correction of the structure factor and use Eq. (11) to obtain the viscosity correction. We now present the details of this computation.

B. Charge fluctuations and the Dean-Kawasaki equation

The local charge density ρ can be determined by computing the fluctuations of the local cation and anion densities, n_+ and n_- , around their mean value c . These fluctuations can be described by the Dean-Kawasaki equation,^{19,20} which has recently been used to compute the conductivity of concentrated electrolytes accurately.²³ It reads

$$\partial_t n_\pm = -\nabla \cdot (n_\pm \mathbf{u}) + D\nabla^2 n_\pm \pm D\nabla \cdot \left(\int d\mathbf{r}' n_\pm(\mathbf{r}) \nabla V(\mathbf{r} - \mathbf{r}') \rho(\mathbf{r}') + \sqrt{2Dn_\pm(\mathbf{r})} \nabla \cdot \zeta_\pm \right), \quad (14)$$

where ζ_+ and ζ_- are uncorrelated white noise fluxes with zero mean and unit variance. The first term on the right-hand side corresponds to advection by the solvent, the second to ion diffusion, the third to ion-ion interactions, and the last one to random Brownian fluctuations.

In what follows, we assume that fluctuations of n_+ and n_- are small compared to the average value c so that we may work at first order in $\delta n_\pm = n_\pm - c$ and ζ_\pm . Since $\rho = n_+ - n_-$ and $\nabla \cdot \mathbf{u} = 0$ due to the fluid being incompressible, we obtain

$$\partial_t \rho = -\mathbf{u} \cdot \nabla \rho + D\nabla^2 \rho + 2cD\nabla \cdot \int d\mathbf{r}' \nabla V(\mathbf{r} - \mathbf{r}') \rho(\mathbf{r}') + \sqrt{4Dc} \nabla \cdot \zeta \quad (15)$$

or, in Fourier space,

$$\partial_t \rho(\mathbf{k}) = \frac{1}{(2\pi)^3} \int d\mathbf{q} \mathbf{u}(\mathbf{k} - \mathbf{q}) \cdot i\mathbf{q} \rho(\mathbf{q}) - Dk^2 \rho(\mathbf{k}) - D\kappa_D^2 \rho(\mathbf{k}) - i\sqrt{4Dc} \zeta. \quad (16)$$

Note that we made use of the fact that the sum of two Gaussian vectors itself is a Gaussian vector, with additive variance, and that $V(q) = 4\pi\ell_B/q^2$ in the case of point-like ions. We also introduced the inverse Debye length $\kappa_D = \lambda_D^{-1}$.

The last equation can be seen as an evolution equation of the form

$$\partial_t \rho = (-\mathbf{a} + i\mathcal{L}) \cdot \rho + \mathbf{b}, \quad (17)$$

where ρ is the vector $\{\rho(\mathbf{k})\}_{\mathbf{k}}$ and the operators \mathbf{a} , \mathbf{b} , and \mathcal{L} are given by

$$\mathbf{a} = \text{diag} \{ Dk^2 + D\kappa_D^2 \}_{\mathbf{k}}, \quad (18)$$

$$\mathbf{b} = \left\{ -i\sqrt{4Dc} \zeta(\mathbf{k}) \right\}_{\mathbf{k}}, \quad (19)$$

$$\mathcal{L} \cdot f(\mathbf{k}, \mathbf{k}') = \frac{1}{(2\pi)^3} \int d\mathbf{q} \mathbf{u}(\mathbf{k} - \mathbf{q}) \cdot \mathbf{q} f(\mathbf{q}, \mathbf{k}'). \quad (20)$$

We may now integrate Eq. (16) over time, assuming that the initial condition vanishes,

$$\rho(\mathbf{k}, t) = \left[\int_0^t e^{(-\mathbf{a} + i\mathcal{L})(t-s)} \cdot \mathbf{b} ds \right]_{\mathbf{k}}. \quad (21)$$

The charge structure factor can now be obtained as

$$\Gamma_\rho(\mathbf{k}, \mathbf{k}'; t) = \left\langle \rho(t) \cdot \rho^\dagger(t) \right\rangle_{\mathbf{k}\mathbf{k}'} = \int_0^t ds \int_0^t ds' e^{(-\mathbf{a} + i\mathcal{L})(t-s)} \times \left\langle \mathbf{b} \cdot \mathbf{b}^\dagger \right\rangle \cdot e^{(-\mathbf{a} - i\mathcal{L}^\dagger)(t-s)}. \quad (22)$$

Since we are interested in static correlations, we now take the limit $t \rightarrow \infty$ and use the fact that

$$\langle \zeta(\mathbf{k}, t) \zeta(\mathbf{k}', t') \rangle = (2\pi)^3 \delta(\mathbf{k} + \mathbf{k}') \delta(t - t'). \quad (23)$$

We obtain (see Ref. 25)

$$(-\mathbf{a} + i\mathcal{L}) \cdot \Gamma_\rho + \Gamma_\rho \cdot (-\mathbf{a} - i\mathcal{L}^\dagger) = -4Dck^2 (2\pi)^3 \delta(\mathbf{k} + \mathbf{k}') \quad (24)$$

or, using the definition of \mathcal{L} and \mathbf{a} ,

$$D(k^2 + k'^2 + 2\kappa_D^2) \Gamma_\rho(\mathbf{k}, \mathbf{k}') - \frac{i}{(2\pi)^3} \int d\mathbf{q} \mathbf{u}(\mathbf{k} - \mathbf{q}) \cdot \mathbf{q} \Gamma_\rho(\mathbf{q}, \mathbf{k}') + \frac{i}{(2\pi)^3} \int d\mathbf{q} \mathbf{u}(\mathbf{k}' - \mathbf{q}) \cdot \mathbf{q} \Gamma_\rho(\mathbf{k}, \mathbf{q}) = 4Dck^2 (2\pi)^3 \delta(\mathbf{k} + \mathbf{k}'). \quad (25)$$

Equation (25) cannot be solved directly. However, since we only wish to compute $\langle \mathbf{f} \rangle$ up to linear order in the velocity field \mathbf{u} , one may use a perturbative approach, which we now describe. At zeroth order in \mathbf{u} , one may set \mathcal{L} and obtain

$$\Gamma_\rho^0(\mathbf{k}, \mathbf{k}') = (2\pi)^3 \delta(\mathbf{k} + \mathbf{k}') \frac{2ck^2}{k^2 + \kappa_D^2} = (2\pi)^3 \delta(\mathbf{k} + \mathbf{k}') g(k). \quad (26)$$

To obtain the correction at first order in \mathbf{u} , one may simply replace Γ_ρ by Γ_ρ^0 in all convolutions in Eq. (25). We obtain

$$\Gamma_\rho(\mathbf{k}, \mathbf{k}') = \Gamma_\rho^0(\mathbf{k}, \mathbf{k}') - \frac{\mathbf{u}(\mathbf{k} + \mathbf{k}') \cdot (i\mathbf{k}' g(k') - i\mathbf{k} g(k))}{D(k^2 + k'^2 + 2\kappa_D^2)}. \quad (27)$$

Inserting this result into Eq. (11) then yields

$$\langle \mathbf{f}(\mathbf{k}) \rangle = \frac{k_B T}{(2\pi)^2 D} 2\ell_B \int d\mathbf{q} \frac{g(q) - g(\mathbf{k} - \mathbf{q})}{q^2 + (\mathbf{k} - \mathbf{q})^2 + 2\kappa_D^2} \frac{\mathbf{q}\mathbf{q}}{q^2} \cdot \mathbf{u}(\mathbf{k}). \quad (28)$$

Note that we have used the incompressibility condition $\mathbf{u}(\mathbf{k}) \cdot \mathbf{k} = 0$. To compute this integral, we use spherical coordinates (q, θ, ϕ) to describe the Fourier space, with \mathbf{k} being the reference for angles. We have

$$\frac{\mathbf{q}\mathbf{q}}{q^2} = \begin{pmatrix} \cos^2 \theta & \sin \theta \cos \theta \cos \phi & \sin \theta \cos \theta \sin \phi \\ \sin \theta \cos \theta \cos \phi & \sin^2 \theta \cos^2 \phi & \sin^2 \theta \sin \phi \cos \phi \\ \sin \theta \cos \theta \sin \phi & \sin^2 \theta \sin \phi \cos \phi & \sin^2 \theta \sin^2 \phi \end{pmatrix}. \quad (29)$$

The rest of the integrand does not depend on ϕ , so we can write

$$\int_0^{2\pi} d\phi \frac{\mathbf{q}\mathbf{q}}{q^2} = \pi \begin{pmatrix} 2 \cos^2 \theta & 0 & 0 \\ 0 & \sin^2 \theta & 0 \\ 0 & 0 & \sin^2 \theta \end{pmatrix}. \quad (30)$$

Note that the first diagonal coefficient is irrelevant since we only wish to evaluate the tensor on a vectorial subspace orthogonal to \mathbf{k} due to incompressibility. Since we interpret \mathbf{f} as a viscous force, we are interested in its long wavelength limit $k \rightarrow 0$ [see Eq. (13)]. Expanding to second order in k and integrating over θ , we obtain

$$\begin{aligned} \langle \mathbf{f}(\mathbf{k}) \rangle &\simeq -\frac{k_B T}{D} \ell_B \frac{2}{15\pi} c \int_0^\infty dq \kappa_D^2 q^2 \frac{5\kappa_D^2 - q^2}{(\kappa_D^2 + q^2)^4} k^2 \mathbf{u}(\mathbf{k}) \\ &= -\frac{k_B T}{D} \ell_B c \frac{1}{60\kappa_D} k^2 \mathbf{u}(\mathbf{k}). \end{aligned} \quad (31)$$

Comparing with Eq. (13), we find that, indeed, electrostatic interactions between ions effectively increase the fluid's viscosity by

$$\Delta\eta_{\text{ion-ion}} = \frac{1}{60\sqrt{8\pi}} \frac{k_B T}{D} \sqrt{\ell_B c}, \quad (32)$$

which corresponds to the Falkenhagen limiting law.¹¹

C. General case: Universal link between the charge structure factor and the viscosity increment

The above Fourier-space approach has the advantage of being computationally lighter than Falkenhagen's historical real-space derivation (which made extensive use of spherical harmonics) and of offering a straightforward way of extending the result to any desired accuracy, provided that the charge structure factor in the absence of flow Γ_ρ^0 is known, and might deviate from Eq. (26) due to non-Coulombic interactions between ions, e.g., short-distance repulsion. In the case of a generic interaction potential $V(\mathbf{k})$, due to translation invariance in the absence of external flow, Γ_ρ^0 can always be written as

$$\Gamma_\rho^0(\mathbf{k}, \mathbf{k}') = 2c(2\pi)^3 \delta(\mathbf{k} + \mathbf{k}') C_\rho^0(\mathbf{k}), \quad (33)$$

where we introduced the rescaled structure factor $C_\rho^0(k)$. One can then express the viscosity increment as a function of this quantity alone,

$$\begin{aligned} \Delta\eta &= \lim_{k \rightarrow 0} \frac{1}{(2\pi)^3 k^2} \frac{k_B T}{D} \int d\mathbf{q} V(\mathbf{q}) \\ &\times \frac{C_\rho^0(\mathbf{q}) - C_\rho^0(\mathbf{k} - \mathbf{q})}{(\mathbf{k} - \mathbf{q})^2 C_\rho^0(\mathbf{q}) + q^2 C_\rho^0(\mathbf{k} - \mathbf{q})} C_\rho^0(\mathbf{q}) C_\rho^0(\mathbf{k} - \mathbf{q}) \mathbf{q}\mathbf{q}. \end{aligned} \quad (34)$$

If we assume ions to be perfectly spherical, then $C_\rho^0(\mathbf{k})$ only depends on k . This assumption is valid for atomic ions (Na^+ , Cl^- , etc.) and is an approximation in the case of molecular ions (SO_4^{2-} , NO_3^- , etc.). We can, therefore, expand the integrand for $k \rightarrow 0$ and perform the integral of ϕ and θ , yielding

$$\Delta\eta_{\text{ion-ion}} = \frac{c}{15(2\pi)^2} \frac{k_B T}{D} \int dq V(q) \frac{d}{dq} \left[q^2 C_\rho^0(q) \frac{\partial C_\rho^0}{\partial q} \right]. \quad (35)$$

In the above case where ions interact through electrostatics alone, with no short-range repulsion, the rescaled structure factor is given by

$$C_\rho^0(k) = \frac{k^2}{k^2 + \kappa_D^2}, \quad (36)$$

and Eq. (35) is equivalent to Eqs. (13) and (32). However, Eq. (36) only provides a very rough estimate of the electrolyte's structure factor, which can be determined from numerical simulations or experiments. For example, Fig. 4(a) shows a comparison between Eq. (36) (red line) and results from molecular dynamics simulations of a concentrated NaCl solution²⁶ (blue circles). The above *Ansatz* fails at capturing the layered structure of ionic correlations at high concentrations, as those emerge from short-distance repulsions between ions.

Consequently, a straightforward way of improving Falkenhagen's result is to use a more precise *Ansatz* for $C_\rho^0(k)$ and insert it into Eq. (35). Although this *Ansatz* does not need to be physically motivated as long as it faithfully reproduces experimental and numerical data, we report results to this end in Sec. II D, making use of a simple model first introduced by Ref. 22.

D. Finite ion size and truncated Coulomb potential

Introducing a short-distance repulsion between ions in the Dean-Kawasaki equation unfortunately makes the computation intractable. However, Avni and co-workers suggested an alternative approach to account for the finite size of ions:²² truncating the Coulomb potential at some finite cutoff distance a , and setting the ion-ion interaction to zero below a [see Fig. 4(b)],

$$V(r) = \frac{\ell_B}{r} \rightarrow \frac{\ell_B}{r} H(r - a), \quad (37)$$

with H being the Heaviside step function. In Fourier space, this corresponds to

$$V(k) = 4\pi \frac{\ell_B}{k^2} \rightarrow 4\pi \frac{\ell_B}{k^2} \cos ka. \quad (38)$$

While this constitutes an apparently uncontrolled approximation, this trick generally yields accurate results, at very little mathematical cost.

Overall, the above derivation of Γ_ρ^0 still holds, replacing κ_D^2 by $\kappa_D^2 \cos ka$ in Eq. (16). The equilibrium structure factor C_ρ^0 is then given by

$$C_\rho^0(k) = \frac{k^2}{\kappa_D^2 \cos ka + k^2}. \quad (39)$$

This result is shown in Fig. 4(a) (yellow line) and captures the essential features of the numerical data. Therefore, truncating the electrostatic potential appears to be a viable strategy to accurately describe the structure of concentrated electrolytes.

Injecting now Eq. (39) into (35), we obtain at leading order in a

$$\Delta\eta_{\text{ion-ion}} = \frac{1}{60\sqrt{8\pi}} \frac{k_B T}{D} \left[\sqrt{\ell_B c} + 6\pi a^2 (\ell_B c)^{3/2} \right]. \quad (40)$$

Equations (35) and (40) constitute the main result of this work.

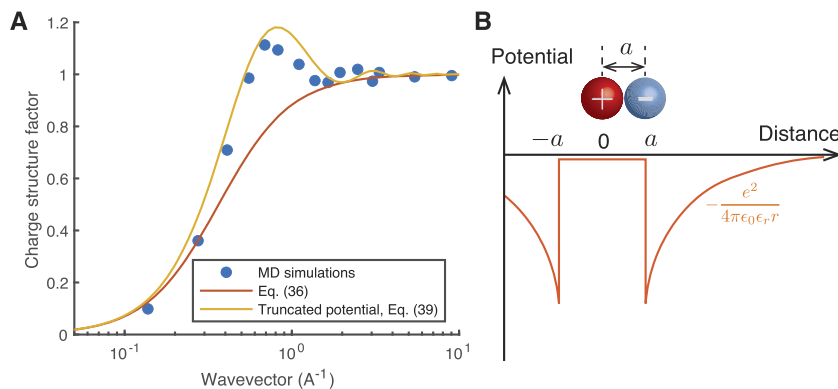


FIG. 4. Effective cutoff electrostatic potential. (a) Charge structure factor of a concentrated electrolyte. Blue points: Molecular dynamics simulation of a solution of NaCl with concentration $c = 1.23\text{M}$ (adapted from Ref. 26). Red line: Eq. (26) (no cutoff). Yellow line: Eq. (39) (cutoff $a = 3\text{Å}$). (b) Definition of the short-distance cutoff a . a corresponds roughly to the distance of minimal approach between two ions: instead of introducing a short-distance repulsion, the interaction potential is simply truncated below a .

E. Multivalent ions and asymmetric salts

In Secs. II A–II D, we only considered the case of a monovalent binary electrolyte X^+, Y^- . However, the discussion can be extended in a straightforward manner to multivalent salts of the type $z : 1$ or $z : z$ with $z > 1$. Noticing that $\rho = z_+n_+ - z_-n_-$, all the above derivations can be redone, yielding

$$\Delta\eta = \frac{1}{60\sqrt{8\pi}} \frac{k_B T}{D} \left[\sqrt{z\bar{z}\ell_B c} + 6\pi a^2 (z\bar{z}\ell_B c)^{3/2} \right], \quad (41)$$

with $\bar{z} = z$ or $(z+1)/2$ depending on $z : z$ or $z : 1$ salt, respectively.

In a similar manner, the case where cations and anions have different diffusion coefficients, say D_+ and D_- , can also be treated analytically; see Refs. 11 and 23. It can be shown that all the above computations still hold, replacing the quantity D by an effective coefficient,

$$D_{\text{eff}} = \frac{(z_+ + z_-)D_+D_-}{D_+z_- + D_-z_+ - 4z_+z_- \left(\frac{D_+ - D_-}{\sqrt{D_+ + D_-} \sqrt{z_+ + z_-} + \sqrt{D_+z_+ + D_-z_-}} \right)^2}. \quad (42)$$

In the above derivation, we also used the same cutoff distance a for cation–cation, cation–anion, and anion–anion interactions. One could, in principle, define specific values of a for cation–cation and anion–anion interactions and then use mixing rules for cross-interactions. Doing so has been reported to only marginally affect the results;²³ therefore, we use a single value of a for all types of interactions.

F. Discussion of the cutoff potential

Finally, let us comment on the choice of the cutoff potential. While the combination of the cutoff potential and the stochastic density functional theory has been shown to be quite powerful to account for finite size effects in the transport dynamics of concentrated electrolytes,²² recent developments²⁴ have suggested that details of the cutoff potential may need to be chosen carefully. In

particular, Ref. 24 suggests setting the potential to some finite value v_0 (which may be positive or negative) at distances smaller than a ,

$$V(r) = \frac{\ell_B}{r} H(r-a) + v_0 H(a-r). \quad (43)$$

In this case, it can be shown that the ion–ion correlator becomes

$$C_\rho^0(k) = \frac{k^2}{k^2 + \kappa_D^2 \cos ka + v_0 \kappa_D^2 (\sin ka - ka \cos ka) / \ell_B k}. \quad (44)$$

Inserting again this result into Eq. (7), we obtain

$$\Delta\eta = \frac{k_B T \sqrt{\ell_B c}}{60D\sqrt{8\pi}} \left[1 + 6\pi a^2 \left[1 - \frac{2}{3} \frac{av_0}{\ell_B} \right] \ell_B c \right], \quad (45)$$

which is identical to the previous result, with a being effectively replaced by $a\sqrt{1 - 2av_0/3\ell_B}$.

Since we can *a priori* expect v_0 to be at most of the order of ℓ_B/a , this modification essentially amounts to modifying a by a factor of order unity. Our results should, therefore, not depend too much on the exact details of the cutoff potential. In what follows, we come back to the simple case where $v_0 = 0$ and, instead, treat a as an adjustable parameter.

III. INTERPRETATION AND COMPARISON WITH EXPERIMENTAL DATA

A. Physics of the ionic viscosity and the truncated potential

At the semi-quantitative level, one can interpret the Falkenhagen limiting law [Eq. (32)] and the existence of a viscosity increment at low concentrations as follows. As previously stated, ions in an electrolyte at equilibrium are typically surrounded by a Debye atmosphere bearing an opposite charge and distributed over a typical length scale λ_D .

Let us now consider the case where an external flow is applied on the electrolyte, with a given velocity gradient $\frac{\partial u}{\partial z}$; see Fig. 1(b).

We notice that, since ions in the correlation cloud are typically separated by λ_D , they will feel different solvent velocities, typically by an amount $\lambda_D \frac{\partial u}{\partial z}(z)$, where $\frac{\partial u}{\partial z}$ is the external velocity gradient. Therefore, an anion in the Debye cloud surrounding a cation will be on average pulled away by a force $\lambda_D \frac{\partial u}{\partial z} / \mu$, where μ is the ion's mobility. The energy landscape of the Debye atmosphere is locally modified by $\Delta E \sim \lambda_D^2 \frac{\partial u}{\partial z} / \mu$ upstream of the flow and by $-\Delta E$ downstream: the probabilities of finding an anion there are modified by $e^{\pm \Delta E / k_B T}$, tilting the cloud along the velocity profile [see Fig. 1(b)]. Since each ion in the correlation cloud is exerting an average force $e^2 / 4\pi\epsilon\lambda_D^2$ on the central cation, the latter overall feels a net force of the order of

$$\frac{\lambda_D^2 \ell_B}{\lambda_D \mu} \left(\frac{\partial u}{\partial z} (+\lambda_D) - \frac{\partial u}{\partial z} (-\lambda_D) \right) \sim \frac{\lambda_D \ell_B}{\mu} \frac{\partial^2 v}{\partial z^2}. \quad (46)$$

Since the electrolyte has a concentration c , the overall force exerted on the liquid is

$$f \sim \frac{c \ell_B \lambda_D}{\mu} \frac{\partial^2 u}{\partial z^2}, \quad (47)$$

which shows that the presence of ions is equivalent to an additional viscosity of the order of

$$\Delta\eta \sim \frac{c \ell_B \lambda_D}{\mu} \sim \frac{1}{\mu} \sqrt{\ell_B c}. \quad (48)$$

Importantly, this simple argument explains why this correction scales as the inverse of the mobility μ , and identifies the quantity $\ell_B c$ as the main relevant parameter.

Furthermore, the use of the truncated potential (38) can be justified from the theoretical point of view by comparing this *Ansatz* to the so-called Poisson–Fermi equation introduced to account for crowding effects in concentrated electrolytes,²⁷

$$(1 - \ell_c^2 \nabla^2) \nabla^2 V = -4\pi \ell_B \rho, \quad (49)$$

where ℓ_c is a measure of the ionic size. Solving Eq. (49) around a point-like charge $\rho = \delta(\mathbf{r})$ and Fourier transforming yields

$$V(k) = \frac{\ell_B}{k^2} \frac{4\pi}{1 + \ell_c^2 k^2} \simeq 4\pi \frac{\ell_B}{k^2} [1 - \ell_c^2 k^2] \simeq 4\pi \frac{\ell_B}{k^2} \cos 2k\ell_c, \quad (50)$$

which corresponds to Eq. (38) with $a = 2\ell_c$, strengthening our otherwise uncontrolled approximation.

Finally, we can interpret the fact that truncating the potential actually results in a larger viscosity correction. The charge structure factor contains terms corresponding to cation–cation, anion–anion, and cation–anion correlations. If no interaction cutoff nor short-distance repulsion is introduced, then nothing prevents oppositely charged ions to significantly overlap each other, being separated by λ_D , which can become smaller than a at high concentrations. If ions overlap, they essentially form a neutral pair that does not interact with the environment and becomes ineffective at transmitting momentum over large distances. Instead, if ions cannot be

TABLE I. Diffusion coefficients of ions at 25 °C.

Ion	D (10^{-9} m ² /s)
Na ⁺	1.33
K ⁺	1.96
Li ⁺	1.03
Ag ₃ ⁺	1.65
Ca ²⁺	0.79
Mg ²⁺	0.705
Ba ²⁺	0.848
Sr ²⁺	0.794
Cd ²⁺	0.717
La ³⁺	0.629
Cl ⁻	2.03
NO ₃ ⁻	1.9
SO ₄ ²⁻	1.07
Br ⁻	2.02

TABLE II. Fitted values of a and original papers of experimental datasets for the studied salts.

Salt	a (Å)	References
NaCl	5.5	32
NaBr	8.5	14 and 18
NaNO ₃	9.0	14
KNO ₃	9.4	14
KF	6.5	32
KBr	5.0	32
KCl	6.5	32
LiCl	6.5	30 and 32
AgNO ₃	6.5	31
CaCl ₂	7.0	14
MgCl ₂	8.0	14
BaCl ₂	5.0	3 and 14
SrCl ₂	8.5	14
LaCl ₃	6.0	14
Na ₂ SO ₄	8.5	14
Cd(NO ₃) ₂	7.5	14

closer than some finite distance a , then interactions are not entirely screened off at high concentrations and the resulting ionic viscosity continues to increase sharply.

B. Comparison with experimental data

In order to assert the validity of our model, we compare our main result (7) [and its equivalent for multivalent salts, see Eq. (41)] to experimental data accessible in the literature. We mainly used the data collected by Isono,¹⁴ who systematically reported the viscosity of a wide variety of electrolytes at temperatures ranging from 15 to 55 °C and for concentrations between 0.05M and the saturation limit. His data unfortunately do not

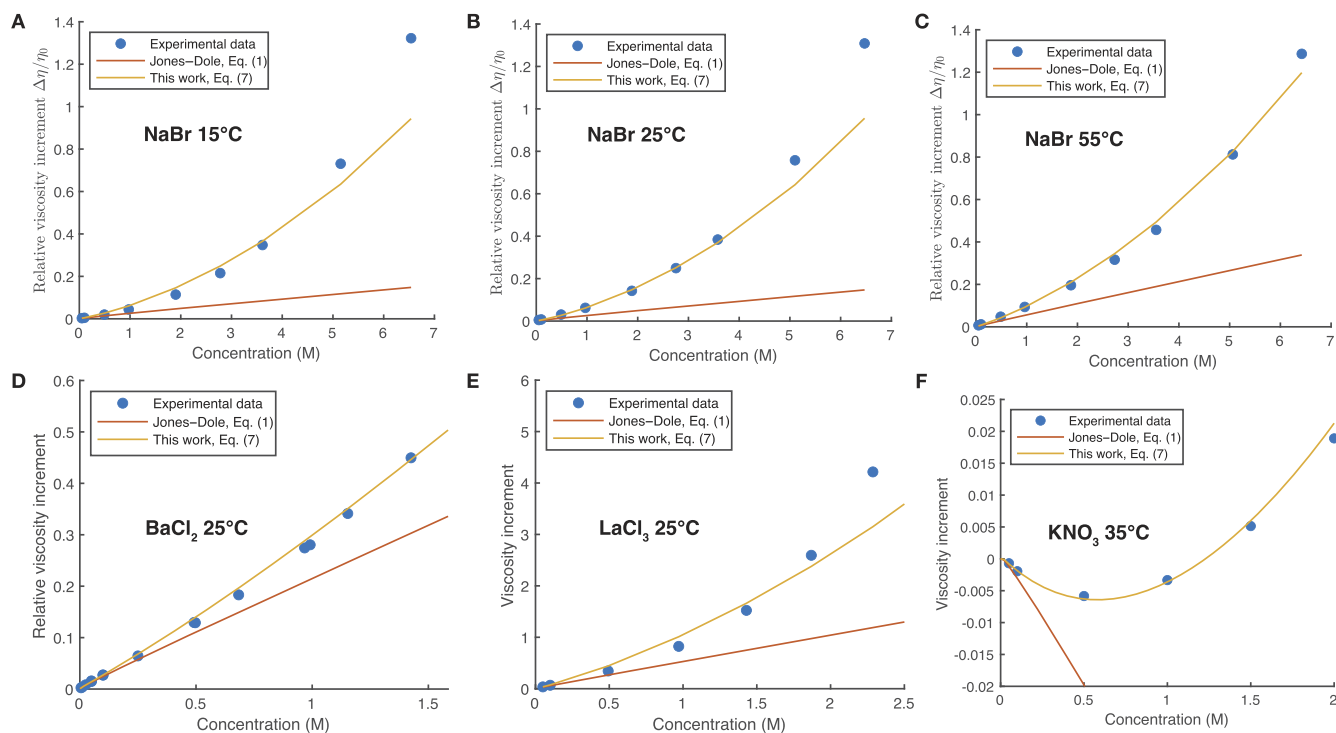


FIG. 5. Comparison between theory [Eq. (7)] and experimental data: effect of temperature and ion valence. Symbols: experimental data for KF, CaCl_2 , and LaCl_3 at 25 °C (a)–(c) and 55 °C (d). [Reproduced with permission from Isono, J. Chem. Eng. Data **29**, 45–52 (1984). Copyright 1984 American Chemical Society and Goldsack and Franchetto, Can. J. Chem. **56**, 1442–1450 (1978). Copyright 1978 Canadian Science Publishing.] Solid line: this work, Eq. (7). Dashed line: Falkenhagen's limiting law, Eq. (32).

contain viscosity values at a very high dilution so that the Falkenhagen regime $\Delta\eta \propto c^{1/2}$ is often difficult to observe (see Fig. 2 for example). The validity of the Falkenhagen limiting law at low concentrations, however, has been discussed elsewhere.^{28,29} In addition, we compared Isono's data to experimental results by other experimentalists.^{18,30–32} No difference was found between the different tested datasets, and nearly all compared favorably to our model.

Overall, we tested Eq. (7) against data for the viscosity of the following salts: NaF, NaCl, NaBr, NaNO_3 , KF, KCl, KBr, KNO_3 , AgNO_3 , LiCl, CaCl_2 , MgCl_2 , BaCl_2 , SrCl_2 , LaCl_3 , Na_2SO_4 , and $\text{Cd}(\text{NO}_3)_2$.

Equation (7) contains three parameters that need to be specified: the Jones–Dole coefficient $B(T)$, the ion diffusion coefficient D , and the short-distance cutoff a .

For the diffusion coefficient, we used tabulated values at infinite dilution (see Table I). Since its values are, in general, different for cations and anions, we used Eq. (42) to determine the value of the effective diffusion coefficient of the electrolyte. It should be noted that the diffusion coefficients of electrolytes are found to also depend on salt concentration;³³ however, these observations are obtained for a coarse-grained definition of the diffusion coefficient. Since we are interested here in the microscopic dynamics of ions, we

assume that at the single-ion level, one may use the limit of infinite dilution.

Since a can be thought of as a minimum approach distance between two ions [see Fig. 4(a)], Avni and co-workers suggested setting a to the sum of the two ionic radii (which can be determined from crystallographic data, for example). This choice, however, compares poorly to experimental data in our case. We found a better agreement for higher values of a , which are more in line with the hydrated diameter. As there is, in addition, an uncertainty on the exact value of a (see Sec. II F), we used a as a fitting parameter independent of temperature (see Table II).

The Jones–Dole coefficient $B(T)$ was determined for each temperature by examining experimental data for low concentrations.

Finally, note that ℓ_B itself depends on T , both directly through Eq. (4) and indirectly through the dielectric constant of water $\epsilon(T)$, which we determined from tabulated data.³⁴ Like the diffusion coefficient, $\epsilon(T)$ is known to depend on salt concentration when measured over macroscopic samples, but since again we use it here to describe the properties of water at the microscopic level around individual ions, we used the value in the absence of salt. Taking this effect into account would amount to describing ion–water interactions and the hydration shell around ions; these are already encapsulated into $B(T)$ and a , respectively.

C. Results and discussion

Overall, we observed a very good agreement between experiments and the model; see Fig. 5. Equation (7) quantitatively matched with the literature data nearly up to the saturation limit, at all tested temperatures [see Figs. 5(a)–5(c)], even for multivalent salts, such as BaCl₂ or LaCl₃ [see Figs. 5(c) and 5(d)].

In most cases, the liquid's viscosity increases with salt concentration. This is not the case for certain salts, such as KCl, KBr, or KNO₃—the viscosity decreases in certain concentration and temperature ranges. This effect, which is more pronounced for salts with large, weakly charged anions, is thought to be caused by interactions between ions and water molecules. It corresponds to negative values of the Jones–Dole coefficient $B(T)$, which are linked to changes in the immediate environment of ions. In particular, salts that decrease the liquid's viscosity tend to be those with low hydration enthalpies (for example, KCl, KBr, and KNO₃—all have hydration enthalpies below 700 kJ/mol³⁵).

Our model is not able to predict which salt should result in a negative viscosity increment, since it does not provide a prediction for the B coefficient. The model, however, correctly predicts that viscosity should increase sharply at high concentrations; see Fig. 5(f) in the case of KNO₃. In particular, the model provides a theoretical justification for the inclusion of an additional term in the Jones–Dole equation, with a $c^{3/2}$ scaling—other usual fitting *Ansätze* often lack a theoretical ground.

The only deviation between the model and experimental data was observed when the Jones–Dole coefficient $B(T)$ changed sign. While a good agreement was obtained for KCl, KBr, and KNO₃ at low temperature [where $B(T) < 0$ for these salts], the model compared poorly to experimental data at higher temperatures, where $B(T) > 0$. As this was only observed for salts for which $B(T)$ changes sign, we can suggest a modification in the hydration shell of the ions to be at the source of this effect, for example. In all other cases, the agreement was good in the entire temperature range.

Finally, we observe that the fitted values of a are, for the most part, well above the ionic radii of the corresponding salts. It should be noted that the “correct” way of defining the ionic size depends on the context; it seems that here one should consider hydrated ions (with typical hydrated radii around 3–4 Å, corresponding to $a \sim 6$ –8 Å).

IV. CONCLUSION

In this work, we derived a theoretical model for the viscosity of concentrated electrolytes. Through the use of a field-theoretical framework based on the Dean–Kawasaki equation, we recovered and considerably extended the long-standing Falkenhagen limiting law, providing a first theoretical insight into the matter beyond the limit of infinite dilution. We showed that fluctuations of charge result in an increase in viscous dissipation, scaling as the salt concentration to the power 1.5 at high concentrations, in contrast to the traditional Jones–Dole equation and similar empirical laws but in excellent agreement with experimental data.

More importantly, we derived a general relation linking the liquid's microscopic structure factor to a macroscopic parameter like viscosity:

$$\Delta\eta_{\text{ion-ion}} = \frac{c}{15(2\pi)^2} \frac{k_B T}{D} \int dq V(q) \frac{d}{dq} \left[q^2 C_p^0(q) \frac{\partial C_p^0}{\partial q} \right]. \quad (51)$$

This result holds in principle regardless of the precise shapes of the charge structure factor C_p^0 or the interaction potential V and would be relevant in other contexts.

The conclusions of our work are twofold: first, it shows the usefulness of the Dean–Kawasaki framework in establishing fluctuation–dissipation relationships in complex contexts, such as concentrated electrolytes. Indeed, direct computations of viscous forces due to electrostatic interactions, in line with Falkenhagen's historical derivation, are particularly arduous and, therefore, only tractable in simple cases, like that of infinite dilution. On the contrary, our approach allows us to link quantities such as the liquid's viscosity to the charge structure factor, a more easily accessible quantity not only in the theory but also in simulations or experiments.^{26,36,37} This observation suggests manifold potential extensions, e.g., by considering the effect of charge or density fluctuations in the solvent as well, or ion transport in more complex environments. In particular, accounting for charge fluctuations in the solvent could allow us to shed light on the effect of ion–water interactions. Another important extension would be to study the effect of solid surfaces. In particular, the presence of surface charges typically results in a local increase in the ion concentration near walls, which could affect the viscosity of electrolytes e.g., in nanometric confinement found in a nanofluidic apparatus or in biological membranes.³⁸

Second, our somewhat formal and general framework does allow us to catch a glimpse of the complexity and the non-universality of ion transport, by allowing for differentiating the behavior of salts with various chemical compositions. While we are, at this stage, unable to fully rationalize specific deviations that certain salts display, we expect that this work will help to further the understanding of ion transport at the nanoscale.

ACKNOWLEDGMENTS

The author thanks Lydéric Bocquet, Baptiste Coquinot, and Mathieu Lizée for fruitful discussions. This project received funding from the European Union's Horizon 2020 research and innovation program under the Marie Skłodowska-Curie Grant Agreement No. 101034413.

AUTHOR DECLARATIONS

Conflict of Interest

The author has no conflicts to disclose.

Author Contributions

Paul Robin: Conceptualization (lead); Formal analysis (lead); Investigation (lead); Writing – original draft (lead); Writing – review & editing (lead).

DATA AVAILABILITY

Data sharing is not applicable to this article as no new data were created. Data supporting the findings of this study are accessible in the literature, as indicated throughout the article.

REFERENCES

- 1 J.-L.-M. Poiseuille, *Ann. Chim. Phys.* **76** (1847).
- 2 A. Sprung, *Experimentelle Untersuchungen über die Flüssigkeitsreibung bei Salzlösungen* (Verlag nicht ermittelbar, 1876).
- 3 G. Jones and M. Dole, “The viscosity of aqueous solutions of strong electrolytes with special reference to barium chloride,” *J. Am. Chem. Soc.* **51**, 2950–2964 (1929).
- 4 P. Debye and E. Hückel, “Zur theorie der elektrolyte. II. Das grenzgesetz für die elektrische leitfähigkeit,” *Phys. Z.* **24**, 305–325 (1923).
- 5 L. Onsager, “Zur theorie der elektrolyte. I,” *Phys. Z.* **27**, 35 (1926).
- 6 A. Chandra and B. Bagchi, “Ionic contribution to the viscosity of dilute electrolyte solutions: Towards a microscopic theory,” *J. Chem. Phys.* **113**, 3226–3232 (2000).
- 7 N. Kavokine, R. R. Netz, and L. Bocquet, “Fluids at the nanoscale: From continuum to subcontinuum transport,” *Annu. Rev. Fluid Mech.* **53**, 377–410 (2021).
- 8 P. Robin and L. Bocquet, “Nanofluidics at the crossroads,” *J. Chem. Phys.* **158**, 160901 (2023).
- 9 C. Angell and E. Sare, “Glass-forming composition regions and glass transition temperatures for aqueous electrolyte solutions,” *J. Chem. Phys.* **52**, 1058–1068 (1970).
- 10 P. Robin, M. Lizée, Q. Yang, T. Emmerich, A. Siria, and L. Bocquet, “Disentangling $1/f$ noise from confined ion dynamics,” *Faraday Discuss.* **246**, 556 (2023).
- 11 H. Falkenhagen and E. Vernon, “LXII. The viscosity of strong electrolyte solutions according to electrostatic theory,” *London, Edinburgh Dublin Philos. Mag. J. Sci.* **14**, 537–565 (1932).
- 12 K. P. Gregory, E. J. Wanless, G. B. Webber, V. S. Craig, and A. J. Page, “The electrostatic origins of specific ion effects: Quantifying the Hofmeister series for anions,” *Chem. Sci.* **12**, 15007–15015 (2021).
- 13 A. A. Chialvo and O. D. Crisalle, “Can Jones–Dole’s B-coefficient be a consistent structure-making/breaking marker? Rigorous molecular-based analysis and critical assessment of its marker uniqueness,” *J. Phys. Chem. B* **125**, 12028–12041 (2021).
- 14 T. Isono, “Density, viscosity, and electrolytic conductivity of concentrated aqueous electrolyte solutions at several temperatures. Alkaline-earth chlorides, lanthanum chloride, sodium chloride, sodium nitrate, sodium bromide, potassium nitrate, potassium bromide, and cadmium nitrate,” *J. Chem. Eng. Data* **29**, 45–52 (1984).
- 15 G. Jones and J. H. Colvin, “The viscosity of solutions of electrolytes as a function of the concentration. VII. Silver nitrate, potassium sulfate and potassium chromate,” *J. Am. Chem. Soc.* **62**, 338–340 (1940).
- 16 L. Onsager and R. M. Fuoss, “Irreversible processes in electrolytes. Diffusion, conductance and viscous flow in arbitrary mixtures of strong electrolytes,” *J. Phys. Chem.* **36**, 2689–2778 (1932).
- 17 M. J. Esteves, M. J. E. d. M. Cardoso, and O. E. Barcia, “A Debye–Hückel model for calculating the viscosity of binary strong electrolyte solutions,” *Ind. Eng. Chem. Res.* **40**, 5021–5028 (2001).
- 18 D. E. Goldsack and R. C. Franchetto, “The viscosity of concentrated electrolyte solutions. II. Temperature dependence,” *Can. J. Chem.* **56**, 1442–1450 (1978).
- 19 K. Kawasaki, “Stochastic model of slow dynamics in supercooled liquids and dense colloidal suspensions,” *Physica A* **208**, 35–64 (1994).
- 20 D. S. Dean, “Langevin equation for the density of a system of interacting Langevin processes,” *J. Phys. A: Math. Gen.* **29**, L613 (1996).
- 21 V. Démery and D. S. Dean, “The conductivity of strong electrolytes from stochastic density functional theory,” *J. Stat. Mech.: Theory Exp.* **2016**, 023106.
- 22 Y. Avni, R. M. Adar, D. Andelman, and H. Orland, “Conductivity of concentrated electrolytes,” *Phys. Rev. Lett.* **128**, 098002 (2022).
- 23 Y. Avni, D. Andelman, and H. Orland, “Conductance of concentrated electrolytes: Multivalency and the Wien effect,” *J. Chem. Phys.* **157**, 154502 (2022).
- 24 O. Bernard, M. Jardat, B. Rotenberg, and P. Illien, “On analytical theories for conductivity and self-diffusion in concentrated electrolytes,” *J. Chem. Phys.* **159**, 164105 (2023).
- 25 R. Zwanzig, *Nonequilibrium Statistical Mechanics* (Oxford University Press, 2001).
- 26 J. Kim, G. Pireddu, I. Chubak, S. Nair, B. Rotenberg *et al.*, *Electrical Noise in Electrolytes: A Theoretical Perspective* (Faraday Discussions, 2023).
- 27 M. Z. Bazant, B. D. Storey, and A. A. Kornyshev, “Double layer in ionic liquids: Overscreening versus crowding,” *Phys. Rev. Lett.* **106**, 046102 (2011).
- 28 W. Cox and J. Wolfenden, “The viscosity of strong electrolytes measured by a differential method,” *Proc. R. Soc. London, Ser. A* **145**, 475–488 (1934).
- 29 J. Anderson, “The Debye–Falkenhagen effect: Experimental fact or friction?,” *J. Non-Cryst. Solids* **172–174**, 1190–1194 (1994).
- 30 I. M. Abdulagatov, A. B. Zeinalova, and N. D. Azizov, “Experimental viscosity B-coefficients of aqueous LiCl solutions,” *J. Mol. Liq.* **126**, 75–88 (2006).
- 31 A. Campbell, A. Gray, and E. Kartzmark, “Conductances, densities, and fluidities of solutions of silver nitrate and of ammonium nitrate at 35°,” *Can. J. Chem.* **31**, 617–630 (1953).
- 32 D. Out and J. Los, “Viscosity of aqueous solutions of univalent electrolytes from 5 to 95 °C,” *J. Solution Chem.* **9**, 19–35 (1980).
- 33 V. Vitagliano and P. A. Lyons, “Diffusion coefficients for aqueous solutions of sodium chloride and barium chloride,” *J. Am. Chem. Soc.* **78**, 1549–1552 (1956).
- 34 C. Malmberg and A. Maryott, “Dielectric constant of water from 0 to 100 °C,” *J. Res. Natl. Bur. Stand.* **56**, 1–8 (1956).
- 35 D. W. Smith, “Ionic hydration enthalpies,” *J. Chem. Educ.* **54**, 540 (1977).
- 36 I. Kalcher and J. Dzubiella, “Structure-thermodynamics relation of electrolyte solutions,” *J. Chem. Phys.* **130**, 134507 (2009).
- 37 W. Kunz, P. Calmettes, G. Jannink, L. Belloni, T. Cartailier, and P. Turq, “The charge structure factor of a 1-1 electrolyte in solution,” *J. Chem. Phys.* **96**, 7034–7038 (1992).
- 38 L. Bocquet and E. Charlaix, “Nanofluidics, from bulk to interfaces,” *Chem. Soc. Rev.* **39**, 1073–1095 (2010).